

# Ground-Truth Validation of the Motion Suspension System for the Qualification of Space Robotic Manipulators

Ferdinand Elhardt<sup>1</sup>, Andreas Stemmer<sup>1</sup>, Manfred Schedl<sup>1</sup>,  
Marco De Stefano<sup>1</sup>, Tobias Bruckmann<sup>2</sup>, and Maximo A. Roa<sup>1</sup>

**Abstract**—Future space missions, including satellite life extension, orbital asset inspection, and deorbiting, rely heavily on space robotic manipulators. However, testing these robots on Earth presents significant challenges, as they are designed to operate in zero gravity but must be tested under 1 g conditions. Since the joints of most space manipulators cannot support their own weight under Earth gravity, mechanical support systems are required to reduce the gravitational joint loads. The Institute of Robotics and Mechatronics at the German Aerospace Center (DLR) and the University of Duisburg-Essen have developed the Motion Suspension System (MSS) – a cable-driven parallel robot that enables ground-based testing of space robotic manipulators in a fully three-dimensional workspace. This paper presents a quantitative assessment of force reconstruction accuracy, for ground-truth validation of the MSS. Using optical motion capture, we achieved sub-degree accuracy in measuring suspension force direction, identifying systematic errors and improving system performance by 15.6 %. This study is crucial to validate the MSS as a qualification platform for space robotic manipulators.

## I. INTRODUCTION

As space missions become more complex, robotic manipulators play increasingly critical roles in In-Space Operations and Services (ISOS) tasks [1], [2], [3]. Already today, robotic manipulators such as the Canadarm2 support docking maneuvers, assembly tasks, and maintenance operations [4].

Verification and validation of these systems are crucial. Once deployed, maintenance becomes a difficult or even impossible task. However, testing these systems on Earth presents a fundamental challenge. [5]. Orbital and most planetary robotic arms are designed to operate in zero or low gravity, but must be tested under the influence of Earth's gravity. Furthermore, robotic arms designed directly for the space application typically have limitations for on ground testing, as they cannot withstand their own weight in Earth's gravity [1].

The most commonly used test facilities [6] for non-gravity-bearing robotic arms are based on a thin layer of air that is pressed between the space asset and a flat floor. An example of these so-called *planar air-bearings* [7] is the *Orbital Robotics Lab* at *ESA ESTEC* [8]. It provides nearly friction-less two-dimensional motions, limited only by the accuracy of the floor's flatness. However, this method does not allow the robotic arm to perform three-dimensional motions which are necessary for more complex operations, such

<sup>1</sup>Institute of Robotics and Mechatronics, German Aerospace Center (DLR), Muenchener Strasse 20, 82234 Oberpfaffenhofen-Wessling, Germany name.surname@dlr.de

<sup>2</sup>Chair of Mechatronics, University of Duisburg-Essen, 47048 Duisburg, Germany

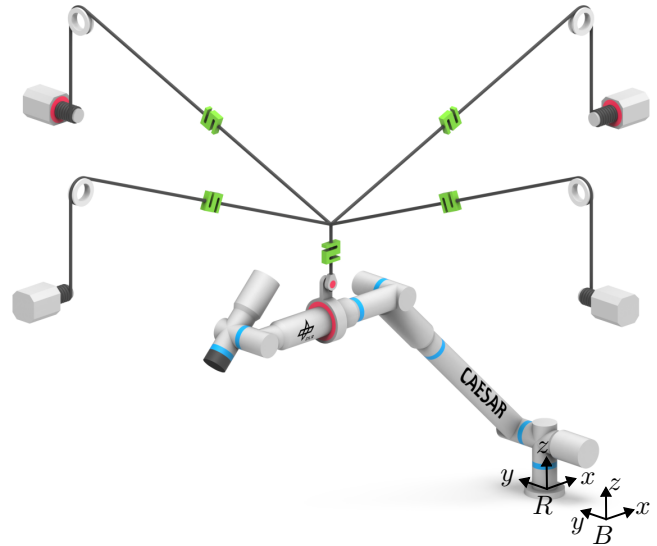


Fig. 1. The MSS is a cable-driven parallel robot to support space manipulators under gravity. The laboratory frame is represented with  $B$  and the robot base with  $R$ . In this case, it supports the DLR space manipulator CAESAR [17], a serial robot arm.

as grasping, vision-based approaches, or collision avoidance maneuvers.

Other methods compatible with motions in all six degrees of freedom include helium balloons [9], often used for system-level testing of solar arrays at satellite production sites. Underwater neutral buoyancy tests [10], [11] are used for astronaut training. However, these methods are strongly affected by hydrodynamic effects or high inertia [6]. Actual zero gravity is provided by free-fall towers and parabolic flights [12], but only for very few seconds. Rail-based suspension systems [13], [14] usually employ gantry cranes for force compensation and come with heavy structure, low mechanical modes, and strong friction effects [15].

To mitigate these drawbacks, the *Institute of Robotics and Mechatronics* at German Aerospace Center (DLR) and the *Chair of Mechatronics* at the *University of Duisburg-Essen* have developed the Motion Suspension System (MSS) [16], shown in Figure 1.

The MSS is a cable-driven parallel robot designed to reduce the gravitational joint loads of space robotic arm systems through active suspension. The guiding principle is joint load minimization rather than zero-gravity simulation: by applying optimized suspension forces, the MSS reduces torques in the manipulator's joints. A suitable algorithm com-

putes the suspension forces by formulating an optimization problem designed to minimize the joint torques of the space robotic arm [18]. This also takes into account the changing center of gravity of the space manipulator during motion.

It was designed for allowing a 6 degree of freedom work envelope, high observation capability, and usability [19]. Cable-driven parallel robots are commonly used in various fields such as automated construction [20], [21], [22], logistics [23], [24], or human rehabilitation [25] due to their lightweight design, large workspace, and exceptional dynamics [26]. Cable-driven parallel robots are based on cables connected to a mobile platform that can be spatially moved. The cables are guided by pulleys and actuated by winches.

Previous works on the MSS have analyzed the main impact factors on the MSS performance: Sensor errors play a minor role, while incorrect offsets lead to strong angle deviations [27]. Controller errors [28] affect dynamic motions and depend on the MSS controller parameters. Friction in the coupling interface [29] interferes with the measurement of the applied suspension force, but plays a minor role in the overall error budget. While our previous approaches have addressed suspension system validation, they rely on internal measurements which cannot detect systematic errors within the cable-based kinematics. This hampers the validity of the previous experiments.

This issue is addressed through a comprehensive end-to-end external measurement validation performed in this study. The objective is to develop a ground-truth validation methodology for assessing the accuracy of MSS suspension force reconstruction, with particular emphasis on the directional components of the applied force vector.

The *directional* reconstruction was selected as the primary focus because it exhibits lower reliability compared to *magnitude* reconstruction of suspension forces. Directional measurement represents the most computationally complex variable in the reconstruction process as it results from a sequential chain of multiple computational steps [16], introducing cumulative error propagation. In contrast, the force magnitude component of the reconstructed suspension force is considered more reliable because they are derived directly from calibrated force sensors with established accuracy specifications.

This study addresses the following specific research questions: (1) What is the achievable accuracy of the MSS suspension force reconstruction under realistic operating conditions? (2) How do individual error sources in the coupling interface contribute to the overall suspension force accuracy? (3) Can systematic calibration offsets improve the MSS performance to meet space robotic qualification requirements?

The remainder of this paper is organized as follows: Section II presents the validation methodology, while Section III illustrates the measurement objects, and the optical motion capture setup used for ground-truth data acquisition. Section IV presents the experimental results, including trajectory-based angle measurements and error identifica-

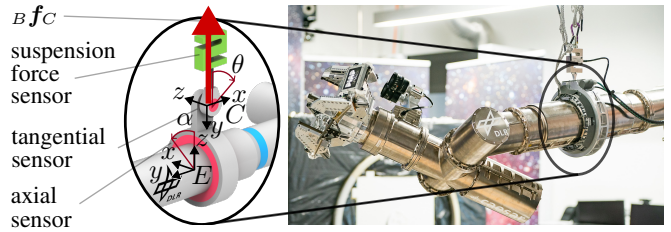


Fig. 2. The coupling interface of the MSS is labeled with the frames  $E$  and  $C$  and is equipped with several sensors for the suspension force reconstruction.

tion with compensation analysis. Section V evaluates the validation method's effectiveness, discusses the identified calibration improvements, and addresses the study's limitations. Finally, Section VI summarizes the key findings and contributions of this ground-truth validation approach for space robotic manipulator qualification.

## II. METHOD

The primarily goal is assessing the accuracy of the reconstructed direction of the suspension force vector  ${}_B\mathbf{f}_C$  (see Figure 2). However, as multiple sensor/model inputs are used in a chain of individual computations (see Equation 1), it makes sense to validate not only the result of the suspension force reconstruction method, but also in-between measurements. This allows to pin-point the individual contributors to the end-to-end error. For these in-between measurements, frame  $R$  (robot base, see Figure 1) and frame  $E$  (MSS-manipulator connection point, see Figure 2) are chosen.

The term *accuracy* is defined as "the closeness of agreement between a test result and the accepted reference value"<sup>1</sup>. In our case, the error between the measured and desired suspension force is denoted with  ${}_B\mathbf{f}_{C,err}$ . The measured suspension force is  ${}_B\mathbf{f}_C$  and the desired suspension force  ${}_B\mathbf{f}_{C,des}$ .

### A. Problem Statement and Assumptions

The MSS supports the CAESAR space robotic manipulator by applying a suspension force which compensates for most of the gravitational influence on the robotic joints. The suspension force is applied via a single connecting cable at the connecting point  $C$  and a two-joint coupling interface at location  $E$ , shown in Figure 2.

To reconstruct the applied force  ${}_B\mathbf{f}_C$  (at point  $C$  with respect to frame  $B$ ) on the space manipulator CAESAR, the force reconstruction method

$${}_B\mathbf{f}_C = \underbrace{\underbrace{{}_B\mathbf{A}_R}_{\text{robot location}} \underbrace{{}_R\mathbf{A}_E}_{\text{robot forward kin.}}}_{\underbrace{{}_B\mathbf{A}_E}_{\text{coupling interface}}} \underbrace{{}_E\mathbf{A}_{E'}(\alpha) \quad {}_{E'}\mathbf{A}_C(\theta)}_{\text{coupling interface}} \underbrace{{}_C\mathbf{f}_C(f)}_{\text{force sensor}} \quad (1)$$

uses available sensor data to reconstruct the suspension force vector. It uses the measured force  $f$  by the suspension force

<sup>1</sup>ISO 3534:20063 <https://www.iso.org/obp/ui/#iso:std:iso:3534:-2:ed-2:v1:en:term:3.3.1>

sensor, the angle  $\alpha$  of the tangential angular sensor and the angle  $\theta$  of the axial angular sensor. Additionally, the forward kinematics of the space manipulator delivers the transformation  ${}^B\mathbf{A}_E$ .

To simplify the equation, we merge dedicated rotation matrices and reformulated to

$${}^B\mathbf{f}_C = {}^B\mathbf{A}_E \cdot {}^E\mathbf{A}_C(\alpha, \theta) \cdot {}^C\mathbf{f}_C(f) \quad (2)$$

While the suspension force magnitude is directly measurable using a force sensor, the measurement of the actual direction of the connection cable between the MSS and CAESAR is more prone to errors. As shown by our previous work [29], friction in the passive joints of the MSS interface mechanism can lead to measurement errors. A ground truth measurement is needed to account for the errors in the MSS measurements.

To understand the motivation behind the measurement in this study, it is crucial to recognize that even small errors in the suspension force direction result in substantial errors in the robot joint torques, potentially compromising the validity of ground-based testing for space robotic applications. As an example, a false angle of  $1.0^\circ$  in the applied suspension force leads to 15.3 N m parasitic torque in the first joint of the manipulator (assuming 350 N suspension force and 2.5 m lever arm). This represents 12% of the nominal joint output torque in the case of CAESAR space manipulator [17] and would introduce a significant error in the joint torque measurement.

Several aspects are explicitly excluded from this validation study. First, the force sensor measurements are assumed to be accurate within manufacturer calibration specifications and are not independently validated. Second, the underlying MSS force computation algorithms based on optimization and kinematic/dynamic models are not assessed. Third, the study does not evaluate the MSS performance under large angular configurations of the robotic segments due to validation measurement principle limitations that restrict accuracy to two degrees of freedom. Additionally, while robot mounting location validation is demonstrated, the primary focus remains on MSS accuracy assessment rather than comprehensive space manipulator performance evaluation. This limitation is justified because the manipulator is considered an exchangeable component within the system architecture.

### B. Validation Concept

The validation concept foresees that MSS measurements are compared with ground-truth validation measurements to assess its accuracy. Hereby, the focus is on the directional components of the applied force vector.

On the one side, the MSS provides the following transformations for the reconstruction:

- ${}^B\mathbf{A}_E \in \mathbb{R}^{3 \times 3}$  as the rotation matrix transforming a vector from laboratory frame  $B$  to the CAESAR coupling frame  $E$ ,
- ${}^E\mathbf{A}_C(\alpha, \theta) \in \mathbb{R}^{3 \times 3}$  as the rotation matrix at CAESAR coupling frame  $E$  taking first the axial and second the tangential joint angle measurements into account,

- ${}^B\mathbf{f}_C$  as the reconstructed suspension force vector.

On the other side, the validation ground-truth measurement (denoted with a bar accent) provides

- ${}^B\bar{\mathbf{A}}_E$  as the rotation from  $B$  to  $E$ ,
- ${}^B\bar{\mathbf{A}}_C$  as the actual suspension force vector orientation,
- ${}^C\bar{\mathbf{f}}_C$  as suspension force from the force sensor, expressed in the  $C$  frame.

The following improves the suspension force reconstruction by adding step-by-step the validation ground-truth measurements. This introduces a series of different suspension force variants from non-compensated to fully-compensated by using ground-truth measurements.

First, the influence of the space manipulator's kinematics is compensated by using  ${}^B\bar{\mathbf{A}}_E$ . Derived from Equation 2, we come to

$${}^B\tilde{\mathbf{f}}_C = \underbrace{{}^B\bar{\mathbf{A}}_E \cdot {}^B\mathbf{A}_E^{-1}}_{{}^B\bar{\mathbf{A}}_{B,corr}} \cdot {}^B\mathbf{A}_E \cdot {}^E\mathbf{A}_C(\alpha, \beta) \cdot {}^C\mathbf{f}_C \quad (3)$$

where  ${}^B\tilde{\mathbf{f}}_C$  is the MSS-specific suspension force reconstruction with removed influence of the space manipulator.

The next step characterizes the error in the MSS reconstruction method coming from the MSS coupling interface, expressed in the correction rotation matrix  ${}^E\bar{\mathbf{A}}_{E,corr}$ :

$${}^B\hat{\mathbf{f}}_C = {}^B\bar{\mathbf{A}}_{B,corr} \cdot {}^B\mathbf{A}_E \cdot {}^E\bar{\mathbf{A}}_{E,corr} \cdot {}^E\mathbf{A}_C(\alpha, \beta) \cdot {}^C\mathbf{f}_C \quad (4)$$

It compensates for systematic errors modeled as constant offsets in the axial and tangential angles of the coupling interface (see Figure 2), expressed in frame  $E$ . Rotation matrices are constructed from measured angles using first-order approximations. Rotation matrices are constructed under the small angle assumption. Cross-coupling terms between sequential rotations are neglected, making the rotation order interchangeable.

To summarize, there are the following variants of the suspension force vectors:

- ${}^B\mathbf{f}_C$ : reconstruction by the MSS
- ${}^B\tilde{\mathbf{f}}_C$ : incl. space manipulator error correction
- ${}^B\hat{\mathbf{f}}_C$ : incl. space manipulator and coupling interface error correction
- ${}^B\bar{\mathbf{f}}_C$ : end-to-end validation measurement

The angle between the suspension force vector and the laboratory reference frame  $B$  is denoted as  $ang_B(\mathbf{f})$  and the suffix  $_{err}$  symbolizes the error compared to the validation measurement.

## III. EXPERIMENTAL SETUP

This section investigates suitable measurement methods for ground-truth validation. The measurement system must satisfy three key requirements: a workspace envelope of 5 m  $\times$  5 m, update rates exceeding 100 Hz to capture fast manipulator motions, and ease of use for repeated experimental setups.

To meet these requirements, we employ a marker-based optical motion capture (MoCap) system (Vicon, Oxford,

UK), which provides high-precision, high-frequency position measurements in controlled indoor environments. The system offers reliable tracking accuracy in the sub-millimeter range, provided that reflective markers remain within the line-of-sight of a calibrated multi-camera setup.

However, the accuracy of angular measurements with this system is influenced by marker placement and measurement object geometry. The suspension force angle directly influences the joint torque of the serial space manipulator. Ideally, an angular accuracy of  $0.007^\circ$  is required, as this corresponds to a torque error of  $0.1\text{ Nm}$  in the first (vertical) joint representing  $0.1\%$  of its  $100\text{ Nm}$  rated torque. However, achieving this level of precision exceeded the capabilities of affordable laboratory instrumentation, as demonstrated in Sec. III-A with the Vicon system. After extensive characterization, the measurement system achieved a repeatable angular accuracy of  $0.3^\circ$ , corresponding to a residual torque of  $4.58\text{ Nm}$  in joint 1. While this represents a significant deviation from the ideal requirement, experimental feasibility necessitated this methodological compromise.

Alternative ground-truth systems were considered but found to be less suitable under the stated constraints, especially by taking into account cost and suitability for other experiments in the laboratory. Ultra-Wideband (UWB) positioning systems, while relatively easy to deploy and robust to occlusions, only offer accuracy in the range of  $10\text{ cm}$  to  $20\text{ cm}$  [30]. Vision-based methods such as visual-inertial SLAM or RGB-D tracking provide infrastructure-free operation but are less robust for texture and lighting conditions and fall short of sub-centimeter demands. Similarly, LIDAR-based localization or fiducial marker tracking (e.g., AprilTags) require extensive calibration and often do not meet the required spatial or temporal resolution. Other active marker localization systems are LED-based, however, direct sunlight (which is needed for other applications) degrades the performance. Electromagnetic-based tracking systems does not reach the required range.

#### A. Measurement Setup

The MoCap system consists of infrared cameras distributed at the ceiling and walls of the laboratory, tracking the 3D position of retroreflective markers via triangulation. The marker arrays need to be placed at corresponding marker array mount objects. The volume was set up by trained personnel to the manufacturer’s procedure, then calibrated and scaled with a calibration process using at minimum 3000 frames. The following specifications are used:

**Measurement Volume:**  $\approx 9\text{ m} \times 5\text{ m} \times 1.5\text{ m}$

**Camera Specification:** 8 Valkyrie V16

**Frame Rate:** 100 Hz

**Object Marker Size:** 14 mm / Pearl Type Markers

**Software / Version:** Vicon Tracker 4.2

In the following, the MoCap marker arrays mounts are discussed, which are placed to measure the measurement objects shown in Figure 3.

#### B. Measurement Objects

Until now, only abstract rotation matrices transforming between frames have been introduced. The following describes the physical locations needed as measurement references at the space manipulator and MSS.

1) *Reference Laboratory Frame B:* The validation measurements by the MoCap system create its own global reference frame  $B_{mocap}$  which is used as reference for all positional/rotational results. As part of the calibration procedure, frame  $B_{mocap}$  was aligned with the laboratory frame  $B$  with an accuracy of less than  $4\text{ mm}$ . By using a laser-based spirit level, the alignment of  $B_{mocap}$  to the gravity vector was confirmed with an accuracy of less than  $0.05^\circ$ .

2) *Robot Mounting Location R:* The robot base frame  $R$  is defined relative to the laboratory frame  $B$  and serves as the root reference for all robot kinematics. It is represented with the transformation  ${}_B\mathbf{A}_R$ . As the robotic setup is fixed-base, the transformation from  $B$  to  $R$  is also rigid. Its alignment with the gravity vector was confirmed by using a spirit level with an accuracy of less than  $0.01^\circ$ .

3) *Robotic Forward Kinematics E:* This is represented by the  ${}_R\mathbf{A}_E$  transformation from robot base frame  $R$  to CAESAR coupling frame  $E$ . To verify this transformation, the robotic segment of the coupling interface mounting (point  $E$  in Figure 2) is selected as measurement object. For this purpose, the dedicated *marker array mount E* was developed which can mechanically interface with a reference plane of the robotic arm, see Figure 3. While a larger distribution of markers is beneficial for the accuracy, we balanced its size with practical aspects such as collisions and calibration possibilities.

Marker array mount objects need to be calibrated such that the object’s MoCap frame is aligned to physical features of the marker array mount. The  $xy$  plane of the MoCap object frame should be aligned to the physical underside surface of the marker array mount. The frame origin and the rotation of the  $z$  axis are arbitrarily chosen.

This calibration was performed by positioning the marker array mount on an aluminum plate that had been leveled using a spirit level with an accuracy of less than  $0.001^\circ$ . The angle around  $x$  and  $y$  axes of the objects MoCap frame were subsequently zeroed in the MoCap software, which aligns the MoCap object frame to MoCap world frame  $B_{mocap}$ .

The validation of the aligning procedure was done by sequentially rotating the marker array mount on the aluminum plate and noting the reported angle in  $x$  and  $y$  axes. A perfectly calibrated object would read zero tilting. In our case, the deviation was  $\pm 0.3^\circ$  which represents the angular accuracy of this marker array mount.

4) *MSS Interface Mechanism and Suspension Force Vector C:* The coupling interface provides the transformation between frame  $E$  and coupling frame  $C$ , represented by  ${}_E\mathbf{A}_C(\alpha, \theta)$ . To perform the validation measurement, we assume that the suspension force vector is aligned with frame  $C$ , which is physically speaking attached to the force sensor. This assumption is valid as the axial and tangential

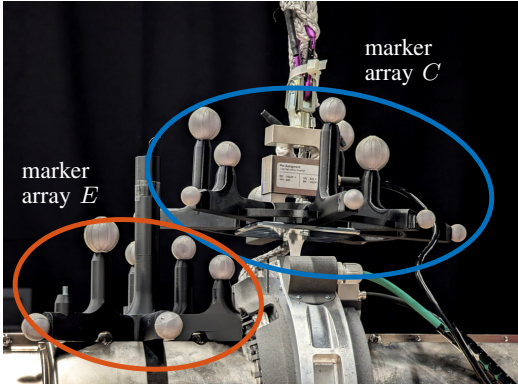


Fig. 3. The two marker array mounts are placed at frame  $E$  and  $C$  to allow the MoCap system to track the orientation.

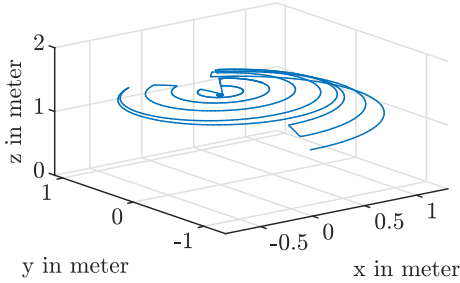


Fig. 4. The experiment trajectory covers an area of  $2.0\text{ m} \times 2.4\text{ m}$  and is circle-shaped with increasing radius.

joints of the coupling interface are passive and due to its low friction, it aligns to the suspension force with an accuracy of less than  $0.054^\circ$  [29].

In order to measure the orientation of frame  $C$ , a dedicated designed MoCap *marker array mount*  $C$  is used, shown in Figure 3. It is equipped with reflective markers to allow tracking by MoCap system. Analog to Section III-B.3, this marker array mount object is calibrated such that the object's MoCap frame is aligned to physical features of the marker array mount. The resulting accuracy is  $\pm 0.1^\circ$ .

### C. Trajectory

For gathering the experimental data, a rotation motion in a horizontal plane was chosen. During the whole trajectory, the suspension force should be vertical, which means that the horizontal components of the suspension force vector should be zero. This is due to marker array mount calibration constraints, where rotation around the  $z$ -axis cannot be measured and is replaced with robotic measurements under the assumption that the marker array mount maintains an approximate upward orientation. The trajectory covers an area of  $2.0\text{ m} \times 2.4\text{ m}$ .

## IV. RESULTS

This section describes the results of the ground-truth measurements. As already stated, this study focuses on the directional components of the reconstruction method. This means that instead of plotting the reconstructed suspension

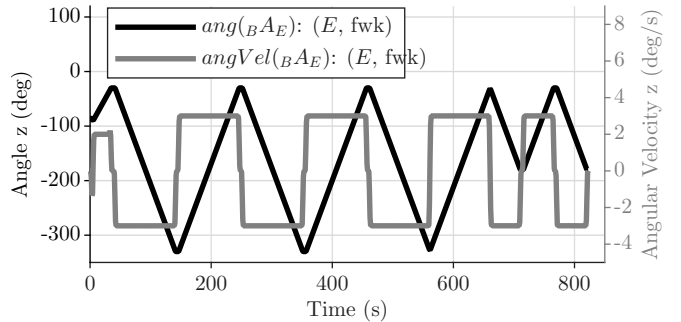
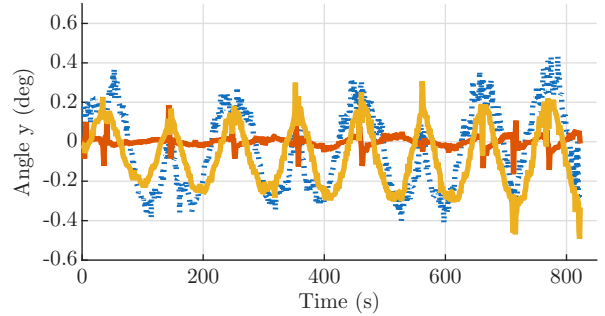
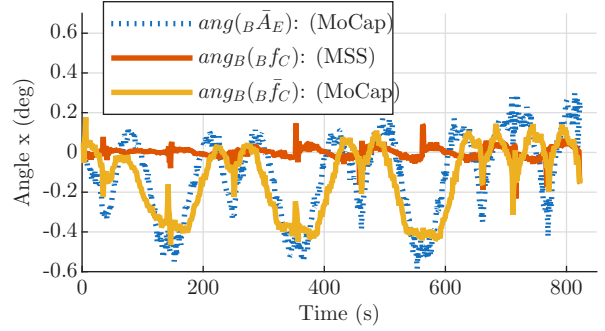


Fig. 5. MSS measurements and validation measurements shown in time domain. All angles are with respect to frame  $B$ .

force vector, the plots show the angle of it. In total, the experiment collected 823 samples.

### A. Trajectory-based Angle Measurements

Figure 5 shows the raw measurements collected during the robotic trajectory. It is distinguished between measurements from the MSS and the validation MoCap system. All values are expressed in the lab frame  $B$ .

The bottom subplot shows the  $z$ -orientation of frame  $E$  as representation of the robot trajectory shown in Figure 4. The rotation is performed between  $-330^\circ$  and  $-30^\circ$ . This is shown for referring the results with respect to the robot's configuration.

The first and second subplot show angles in  $x$  and  $y$  axes. The validation measurement of frame  $E$  by the MoCap system shows  $ang(B, \bar{A}_E)$  which is the angle of frame  $E$  (robot's mounting location of the MSS coupling interface). It is expressed with respect to the laboratory frame  $B$ . This measurement is used for formulating the correction matrix  $B\bar{A}_{B,corr}$  (see Equation 4). The values show a sine-shaped

correlation to the  $z$ -orientation of the space manipulator with an amplitude of  $\approx 0.5^\circ$  for both the  $x$  and  $y$  axes.

The figure also shows  $ang_B(\mathbf{f}_C)$  which is the angle of MSS-reconstructed suspension force with respect to the laboratory frame  $B$ . During constant velocity, the values are in a range of  $\pm 0.01^\circ$  which is below the range of the MSS marker array mount accuracy of  $0.1^\circ$ . At velocity changes (eg at  $t=140$  s,  $240$  s,  $350$  s, ...), the angle shows a peak of  $\approx \pm 0.15^\circ$ . This represents the MSS controller errors which is further analyzed in our previous work [28].

The validation measurement is shown in Figure 5 by  $ang(\mathbf{f}_C)$ , which is the angle of the suspension force measurement by the MoCap system. We use this as ground-truth. In the optimal case, the measured suspension force would match this value. These values follow a sine-shape correlation to the  $z$ -orientation of the space manipulator within a band of  $-0.40^\circ$  to  $0.05^\circ$  for  $x$  and  $-0.28^\circ$  to  $0.15^\circ$ . At velocity changes, there are clear spikes of  $0.1^\circ$  due to controller errors [28]. The velocity at point  $E$  is up to  $0.07 \text{ m s}^{-1}$  (not shown in the plot).

### B. Error Identification and Compensation

While the visualizations above compare MSS reconstruction results with the validation measurements of the MoCap systems, the following focuses on the identification of the angular error introduced by the MSS.

The correction matrix  ${}_{B}\bar{\mathbf{A}}_{B,corr}$  (Equation 3) results from the validation measurement of frame  $E$  and stands for the accuracy of the space manipulator. However, the correction  ${}_{E}\bar{\mathbf{A}}_{E,corr}$  (Equation 4) is more important for this study because it shows the accuracy of the MSS coupling interface. The minimal root mean square (rms) of  ${}_{B}\hat{\mathbf{f}}_{C,err}$  identifies  $\alpha_0 = 0.04^\circ$  and  $\theta_0 = 0.04^\circ$ .

As the angles of the suspension force vector follow a repetitive pattern corresponding to the  $z$  axis orientation, the graph can be simplified by using an angle-domain instead of time-domain. Figure 6 integrates every rotation cycle in one plot, but neglects the circle's radius of the robotic trajectory. The horizontal axis of the plot illustrates the orientation of frame  $E$  with respect to frame  $B$ . The error of the MSS-reconstructed suspension force angle  $ang_B(\mathbf{f}_{C,err})$  shows the error with non-calibrated rotations. Its root mean square error (rmse) over the complete trajectory is  $0.199^\circ$  [ $0.191^\circ$ ,  $0.207^\circ$ ] (95% confidence intervals). A separate analysis (not shown here) indicates that there is no dependency with the MSS velocity in this experiment.

Compensating the space manipulator's error results in  $ang_B(\mathbf{f}_{C,err})$  and reduces the rmse to  $0.0749^\circ$  [ $0.0710^\circ$ ,  $0.0790^\circ$ ] (95% confidence intervals). This shows the performance of the MSS coupling interface without correcting its systematic errors. Finally, the angle  $ang_B(\hat{\mathbf{f}}_{C,err})$  shows the optimized correction of the coupling interface, resulting  $0.0633^\circ$  [ $0.0593^\circ$ ,  $0.0672^\circ$ ] of rmse (95% confidence intervals). This represents an improvement of 15.6% compared to the non-corrected suspension force reconstruction.

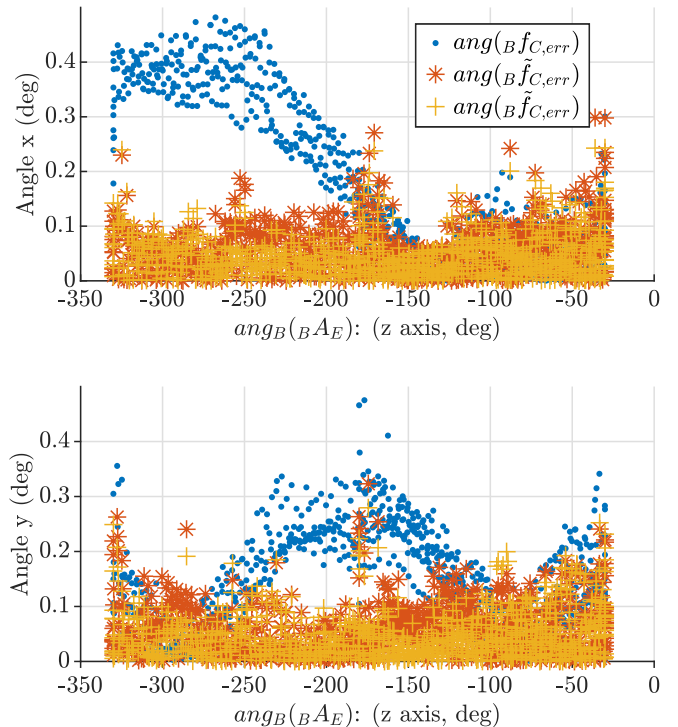


Fig. 6. MSS measurements and validation measurements shown in angular domain. Angles are with respect to frame  $B$ .

## V. DISCUSSION

The objective of this study is to develop a method for validating the accuracy of MSS suspension force reconstruction by utilizing ground-truth data. Hereby, the use of an optical MoCap systems fulfills our requirements for providing ground-truth data. It provides data in dynamic scenarios and with mid-range frequency up to 100 Hz (as comparison: the MSS operates with 1 kHz [16]) and covers the necessary workspace envelope. The accuracy of the measurement setup allows measurements up to  $0.1^\circ$ , which corresponds to  $1.53 \text{ N m}$  residual torque [27] in joint 1 of the space manipulator. In the case of the CAESAR space manipulator, this is 1.91% of the nominal joint output torque which we accept as validation accuracy. However, these systems require extensive calibration procedures for the system itself as well as for the global MoCap frame and the marker array mounts. Every calibration step introduces uncertainties of the measurement method which are considered in this study.

The results show that the performance of the MSS is strongly affected by the accuracy of the forwarded frame  $E$ . While the study includes validation measurements of the *robot mounting location* (frame  $E$ ) it is not its focus. Nevertheless, this shows that the performance of the MSS is strongly dependent on the space manipulator kinematics information.

The used trajectory for this analysis covers a large workspace. The result shows that the accuracy is not significantly dependent on the location in the workspace. However, the trajectory avoids large angles in the analyzed robotic

segments. This is due to the measurement principle, but also limits the significance of the results. For our goal, this limitation is acceptable.

The result of this study identified a calibration offset in the coupling interfaces joints which improves the performance of the MSS by 15.6% compared to the non-corrected suspension force reconstruction. The physical origin of these offsets lies in unavoidable mechanical imperfections such as assembly tolerances and sensor mounting alignment errors. However, this does not hamper the internal measurement of the MSS but rather implies that the calibration of the coupling interface's joints should be improved to identify these offsets, for example by using the motion capture system presented in this study. Importantly, these error sources are inherent to any mechanical suspension system, particularly those involving multi-joint coupling interfaces. The remaining error between MSS-reconstructed and validated suspension force angle is below the accuracy of the validation measurement method. This finding is important as it shows that the internal measurement of the MSS is sufficient.

As a limitation it is worth to mention that this study defines *performance* as the deviation from the desired suspension force. This means that possible errors in the *desired* suspension force cannot be discovered. These errors could result from errors in the MSS force computation [18] which is based on optimization algorithms and kinematic/dynamics information of the space manipulator.

As outlook, the validation measurement method could be improved. While the positional tracking performance of the MoCap system is already at its peak, the angular measurement can be improved by increasing the size of the marker array mount. Other measurement methods can be investigated to increase the measurement accuracy.

## VI. CONCLUSION

As a conclusion we have shown a ground-truth based validation method for the performance of the MSS. It mainly focuses on the suspension force, which is a force vector applied on the space manipulator. The orientation of this suspension force is crucial as it strongly affects the torque in the space manipulator's joints. The performance is defined as deviation from a computed desired suspension force. This study validates the sensors in the MSS coupling interface and the processing of its data. The method is based on an optical MoCap system that allows to measure the orientation of the components of the MSS via reflective markers. The results shows that the offset calibration of the angular sensors in the MSS coupling mechanism needs to be improved, while the incremental measurements are within the requirements. The improvement by the validation is 15.6% and the remaining error is below the validation measurement accuracy.

## REFERENCES

- [1] E. Papadopoulos, F. Aghili, O. Ma, and R. Lampariello, "Robotic Manipulation and Capture in Space: A Survey," in *Frontiers in Robotics and AI*, 2021. DOI: 10.3389/frobt.2021.686723
- [2] "The Space Act: Regulation of the European parliament and of the council on the safety, resilience and sustainability of space activities in the Union," European Commission, 2025.
- [3] R. H. Miller, M. L. Minsky, and D. B. S. Smith, "Space Applications of Automation, Robotics and Machine Intelligence Systems (ARAMIS). Volume 4: Supplement, Appendix 4.3: Candidate ARAMIS Capabilities," NASA, NAS 1.26:162083, 1982.
- [4] G. Gibbs and S. Sachdev, "Canada and the International Space Station program: Overview and status," *Acta Astronautica*, vol. 51, no. 1, pp. 591–600, 2002. DOI: 10.1016/S0094-5765(02)00077-2
- [5] M. De Stefano, H. Mishra, A. M. Giordano, R. Lampariello, and C. Ott, "A Relative Dynamics Formulation for Hardware-in-the-Loop Simulation of On-Orbit Robotic Missions," *IEEE Robotics and Automation Letters*, 2021. DOI: 10.1109/LRA.2021.3064510
- [6] A. Flores-Abad, O. Ma, K. Pham, and S. Ulrich, "A review of space robotics technologies for on-orbit servicing," *Progress in Aerospace Sciences*, 2014. DOI: 10.1016/j.paerosci.2014.03.002
- [7] J. L. Schwartz, M. A. Peck, and C. D. Hall, "Historical Review of Air-Bearing Spacecraft Simulators," *J. of Guidance, Control, and Dynamics*, 2003. DOI: 10.2514/2.5085
- [8] H. Kolvenbach and K. Wormnes, "Recent Developments on On-Orbit, a 3-DOF Free Floating Contact Dynamics Testbed," in *Proc. Int. Symp. on Artificial Intelligence, Robotics and Automation in Space (iSAIRAS)*, Beijing, China, 2016.
- [9] M. Leipold, M. Eiden, C. Garner, L. Herbeck, D. Kassing, T. Niederstadt, T. Krüger, G. Pagel, M. Reza-zad, H. Rozemeijer, W. Seboldt, C. Schöppinger, C. Sickinger, and W. Unckenbold, "Solar sail technology development and demonstration," *Acta Astronautica*, vol. 52, no. 2–6, pp. 317–326, 2–6 2003. DOI: 10.1016/S0094-5765(02)00171-6
- [10] C. Carignan and D. Akin, "The reaction stabilization of on-orbit robots," *IEEE Control Systems Magazine*, 2000. DOI: 10.1109/37.887446
- [11] H. Sawada, K. Ui, M. Mori, H. Yamamoto, R. Hayashi, S. Matunaga, and Y. Ohkami, "Micro-gravity experiment of a space robotic arm using parabolic flight," *Advanced Robotics*, 2004. DOI: 10.1163/156855304322972431
- [12] C. Menon, A. Aboudan, S. Cocuzza, A. Bulgarelli, and F. Angrilli, "Free-Flying Robot Tested on Parabolic Flights: Kinematic Control," *Journal of Guidance, Control, and Dynamics*, vol. 28, no. 4, pp. 623–630, 4 2005. DOI: 10.2514/1.8498
- [13] Brown and J. Dolan, "A Novel Gravity Compensation System for Space Robots," in *Proc. ASCE Specialty Conf. on Robotics for Challenging Environments*, 1994.

- [14] L. K. Dungan, P. S. Valle, D. R. Bankieris, A. P. Lieberman, L. Redden, and C. Shy, "Patent: US9194977B1. Active response gravity offload and method," U.S. Patent 9194977B1, 2015.
- [15] G. White and Yangsheng Xu, "An active vertical-direction gravity compensation system," *IEEE Trans. on Instrumentation and Measurement*, vol. 43, no. 6, pp. 786–792, 6 1994. DOI: 10.1109/19.368066
- [16] F. Elhardt, R. Boumann, M. De Stefano, R. Heidel, P. Lemmen, M. Heumos, C. Jeziorek, M. A. Roa, M. Schedl, and T. Bruckmann, "The Motion Suspension System – MSS: A Cable-Driven System for On-Ground Tests of Space Robots," in *Advances in Mechanism and Machine Science*, M. Okada, Ed., vol. 148, Cham: Springer Nature, 2023, pp. 379–388. DOI: 10.1007/978-3-031-45770-8\_38
- [17] A. Beyer, G. Grunwald, M. Heumos, M. Schedl, R. Bayer, W. Bertleff, B. Brunner, R. Burger, J. Butterfaß, R. Gruber, T. Gumpert, F. Hacker, E. Krämer, M. Maier, S. Moser, J. Reill, M. A. Roa, H.-J. Sedlmayr, N. Seitz, and A. Albu-Schäffer, "CAESAR: Space Robotics Technology for Assembly, Maintenance, and Repair," in *Proc. Int. Astronautical Congress*, Bremen, 2018.
- [18] M. De Stefano, R. Vijayan, A. Stemmer, F. Elhardt, and C. Ott, "A Gravity Compensation Strategy for On-ground Validation of Orbital Manipulators," in *Proc. IEEE Int. Conf. on Robotics and Automation*, London, UK: IEEE, 2023, pp. 11 859–11 865. DOI: 10.1109/ICRA48891.2023.10161480
- [19] F. Elhardt, R. Boumann, M. De Stefano, R. Heidel, P. Lemmen, M. Heumos, C. Jeziorek, M. Roa, M. Schedl, and T. Bruckmann, "System Requirements Elicitation and Conceptualization for a Novel Space Robot Suspension System," in *Proc. Symp. on Advanced Space Technologies in Robotics and Automation (ASTRA)*, Leiden, Niederlande, 2023.
- [20] R. Heidel, P. Lemmen, R. Boumann, and T. Bruckmann, "Design and implementation of a cable-driven robot for automated masonry of building walls," in *Fachtagung VDI Mechatronik*, Darmstadt: VDI, 2022.
- [21] Y. Wu, H. H. Cheng, A. Fingrut, K. Crolla, Y. Yam, and D. Lau, "CU-brick cable-driven robot for automated construction of complex brick structures: From simulation to hardware realisation," in *Proc. IEEE Int. Conf. on Simulation, Modeling, and Programming for Autonomous Robots (SIMPAN)*, Brisbane, QLD, 2018. DOI: 10.1109/SIMPAN.2018.8376287
- [22] K. Iturralde, M. Feucht, D. Illner, R. Hu, W. Pan, T. Linner, T. Bock, I. Eskudero, M. Rodriguez, J. Gorrotxategi, J. B. Izard, J. Astudillo, J. Cavalcanti Santos, M. Gouttefarde, M. Fabritius, C. Martin, T. Henninge, S. M. Nornes, Y. Jacobsen, A. Pracucci, J. Cañada, J. D. Jimenez-Vicaria, R. Alonso, and L. Elia, "Cable-driven parallel robot for curtain wall module installation," *Automation in Construction*, 2022. DOI: 10.1016/j.autcon.2022.104235
- [23] A. Pott, *Cable-Driven Parallel Robots: Theory and Application* (Springer Tracts in Advanced Robotics). Springer, 2018. DOI: 10.1007/978-3-319-76138-1
- [24] N. Pedemonte, T. Rasheed, D. Marquez-Gamez, P. Long, E. Hocquard, F. Babin, C. Fouché, G. Caverot, A. Girin, and S. Caro, "FASTKIT: A Mobile Cable-Driven Parallel Robot for Logistics," in *Advances in Robotics Research*, ser. Springer Tracts in Advanced Robotics, Cham: Springer, 2020, pp. 141–163. DOI: 10.1007/978-3-030-22327-4\_8
- [25] M. Harshe, J.-P. Merlet, D. Daney, and S. Bennour, "A Multi-sensors System for Human Motion Measurement: Preliminary Setup," in *Proc. World Congr. in Mechanism and Machine Science*, 2011.
- [26] M. Zarebidoki, J. S. Dhupia, and W. Xu, "A Review of Cable-Driven Parallel Robots: Typical Configurations, Analysis Techniques, and Control Methods," *IEEE Robotics & Automation Magazine*, 2022. DOI: 10.1109/MRA.2021.3138387
- [27] F. Elhardt, M. De Stefano, M. Schedl, A. Stemmer, T. Bruckmann, and M. A. Roa, "Analysis of Sensor Errors of a Suspension Systems for Space Robots," in *Proc. International Conference on Space Robotics*, Luxembourg, 2024.
- [28] F. Elhardt, A. Stemmer, A. Shu, M. De Stefano, M. Schedl, M. A. Roa, and T. Bruckmann, "Experiment-Based Performance Analysis of the Motion Suspension System for Space Robot Testing," in *Proc. 75th International Astronautical Congress*, Milan, Italy, 2024.
- [29] F. Elhardt, A. Shu, A. Stemmer, M. De Stefano, M. Schedl, M. A. Roa, and T. Bruckmann, "Friction Analysis of the Motion Suspension System for Improved Space Robot Testing," in *2025 IEEE Aerospace Conference*, 2025, pp. 1–9. DOI: 10.1109/AERO63441.2025.11068555
- [30] H. Guo, S. Song, H. Yin, D. Ren, and X. Zhu, "Optimization of UWB indoor positioning based on hardware accelerated Fuzzy ISODATA," *Scientific Reports*, vol. 14, no. 1, p. 17 985, 2024. DOI: 10.1038/s41598-024-68998-0